# Quantum computing with superconducting devices: A three-level SQUID qubit

Zhongyuan Zhou* and Shih-I Chu
*Department of Chemistry, University of Kansas, Lawrence, Kansas 66045*

Siyuan Han
*Department of Physics and Astronomy, University of Kansas, Lawrence, Kansas 66045*

(Received 6 February 2002; published 20 August 2002)

A three-level scheme for implementing single-qubit operations in superconducting quantum interference devices is proposed and analyzed. We show that, compared with the conventional two-level scheme, the proposed three-level qubit scheme is much faster and has a much lower intrinsic error rate.

DOI: 10.1103/PhysRevB.66.054527 PACS number(s): 03.67.Lx, 85.25.Dq, 89.70.+c

## I. INTRODUCTION

The discovery that quantum algorithms are capable of solving certain types of classically intractable problems has stimulated intensive investigations aimed at the physical implementation of quantum computation.[1] The building block of a quantum computer is called a quantum bit, or simply a qubit, from which multiqubit quantum gates can be constructed and networked to perform any desired quantum logic operation.[2,3] An ideal qubit is a quantum two-level system whose state can be prepared and controlled by experimenters. Since a rather large number of qubits is required to build a practically useful quantum computer, it is essential that the physical qubits are readily scalable to form quantum circuits and networks. Furthermore, a key consideration for any type of physical qubit is that the decoherence must be weak to allow fault-tolerant quantum computation.[4,5] Superconducting qubits based on the quantum dynamics of magnetic flux (phase) and/or electric charge have the potential to fulfill both requirements.[6–10] For instance, recent experiments with Josephson-effect-based devices [such as the superconducting quantum interference device (SQUID) and the single Cooper pair box] have not only demonstrated the quantum nature of these superconducting devices, but also that a very weak dissipation can be achieved.[11–17]

However, compared with other qubit candidates (such as trapped ions,[18] nuclear spins,[19] and cavity QED[20]), decoherence presents a much more formidable challenge to superconducting qubits. For a true two-level qubit, decoherence occurs due to the coupling of the qubit to its environment. However, all of the proposed superconducting qubits have multiple energy levels which result in adverse effects on quantum gate operations. This problem is more severe for flux-based qubits of the conventional two-level configuration since the noncomputational states are not well separated from the two computational bases (Fig. 1). In fact, even in the case of an isolated SQUID qubit, coupling between the computational bases $|0\rangle$ and $|1\rangle$ and the states $|n\geqslant 2\rangle$ of the noncomputational subspace results in significant errors for one-qubit gate operations, as in the NOT (bit-flip) and Hadamard gates.[21]

In this work, we study how the properties of one-qubit gate operations, using the NOT gate as a specific example because of its importance to the two-qubit CNOT gate, are adversely affected by the multilevel structure of SQUID's and explore ways to utilize the multilevel structure to circumvent these adverse effects. We show that the conventional method of operating SQUID qubits by generating Rabi oscillations between the levels $|0\rangle$ and $|1\rangle$ using resonant microwave pulses has many fundamental shortcomings. Problems such as intrinsic gate errors (errors that occur even in the absence of decoherence), leakage to noncomputational states (NCS's), and consequently slow gate operations are very difficult to solve with the conventional scheme of two-level SQUID qubits (2LSQ). We demonstrate that these problems can be addressed effectively by making the use of three $\Lambda$-shaped levels of a multilevel rf SQUID qubit, where an auxiliary level $|a\rangle$ is used to significantly increase the speed and reduce errors of quantum gate operations. Recently, a universal scheme of correcting errors due to the off-resonant coupling in a $N$-level qubit has been presented.[22] In this scheme errors are eliminated by applying a sequence of additional $2(N-2)$ rf pulses with frequencies $\omega_{i1}$ and $\omega_{i2}$, $i=3,...,N$, where $\omega_{ij}\equiv(E_i-E_j)/\hbar$, to the qubit. However, in practice this method could be quite difficult to implement in rf SQUID qubits because of the large number of levels, and hence rf pulses, involved. In comparison, the scheme proposed by us requires only two rf pulses with frequencies $\omega_{a1}$ and $\omega_{a2}$ and therefore is much easier to implement experimentally.

## II. SQUID QUBIT

A SQUID consists of a superconducting loop of inductance $L$ interrupted by a Josephson tunnel junction. Applying the resistively shunted junction (RSJ) model,[23] the junction is characterized by its critical current $I_c$, shunt capacitance $C$, and shunt resistance $R$. The classical deterministic equation of motion of such a SQUID is

$$C\ddot{\Phi}+R^{-1}\dot{\Phi}=-\frac{\partial U}{\partial \Phi}, \tag{1}$$

where $\Phi$ is the total magnetic flux enclosed in the SQUID loop. Equation (1) is isomorphic to that of a particle of mass $C$ moving in a one-dimensional potential $U(\Phi)$ with damping coefficient $R^{-1}$. The potential is given by

$$U(\Phi)=\frac{(\Phi-\Phi_e)^2}{2L}-E_J\cos\left(2\pi\frac{\Phi}{\Phi_0}\right), \tag{2}$$

 

where $E_J \equiv I_c \Phi_0 / 2\pi$ is the maximum magnitude of the Josephson coupling energy, $\Phi_e$ is the external magnetic flux applied to the SQUID, and $\Phi_0 \equiv h/2e$ is the flux quantum. In the presence of an external flux the SQUID generates a superconducting current circulating the loop to keep the total number of fluxoids, $f$, in the SQUID quantized. For $x_e \equiv \Phi_e / \Phi_0 = 1/2$, the potential has symmetric double wells. The left (right) well corresponds to the $f=0$ ($f=1$) fluxoid state. Increasing (decreasing) $x_e$ slightly from 1/2 tilts the potential to the right (left), which provides an easy way to control the potential and interwell level separations (Fig. 1).

The Hamiltonian of a SQUID is $H_0(\Phi) = p_\Phi^2/2C + U(\Phi)$, where $p_\Phi \equiv -i\hbar\partial/\partial\Phi$ is the momentum operator conjugate to $\Phi$. By introducing the mass $m = C\Phi_0^2$ and the position $x = \Phi/\Phi_0$ of the "flux" particle, the Hamiltonian can be written as

$$H_0(x) = p_x^2/2m + U(x), \tag{3}$$

with the potential given by

$$U(x) = \frac{1}{2} m\omega_{LC}^2 (x - x_e)^2 - \frac{1}{4\pi^2} m\omega_{LC}^2 \beta_L \cos 2\pi x, \tag{4}$$

where $p_x \equiv -i\hbar\partial/\partial x$, $\omega_{LC} = 1/\sqrt{LC}$ is the characteristic frequency of the SQUID, and $\beta_L \equiv 2\pi L I_c / \Phi_0$. The shape of the potential is determined uniquely by the dimensionless parameter $\beta_L$ and the external flux $x_e$.

The eigenenergies $E_n$ and eigenstates $|n\rangle$ of a SQUID qubit can be obtained by numerically solving the Schrödinger equation with an anharmonic Hamiltonian $H_0(x)$. It has been shown that the eigenstates depend only on the potential shape parameter $\beta_L$ and the characteristic impedance $Z_0 \equiv \sqrt{L/C}$ and that the eigenenergies are scaled to $\hbar\omega_{LC}$.[24] The potential and the energy levels of a SQUID with $Z_0 = 50\ \Omega$ (i.e., $L = 100$ pH and $C = 40$ fF), $\beta_L = 1.20$, and $\omega_{LC} = 5 \times 10^{11}$ rad/s are plotted in Fig. 1 for external flux $x_e = -0.501$. Note that the SQUID's energy level structure can be controlled by adjusting $\beta_L$ and $x_e$. For example, the total number of levels in the two wells, $N_L + N_R$, increases with $\beta_L$, while the difference $N_L - N_R$ increases with $x_e$.

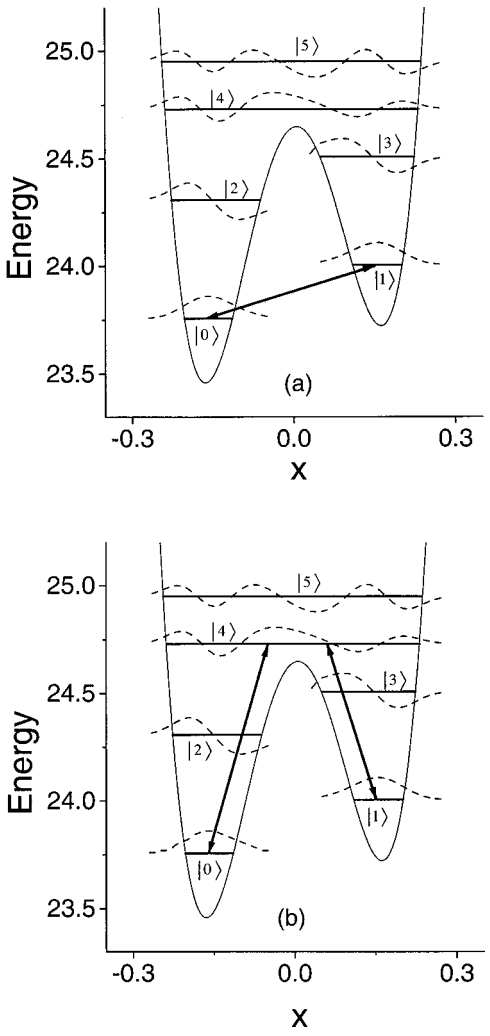


FIG. 1. Potential energy and the first six energy levels of a SQUID with $L = 100$ pH, $C = 40$ fF, and $I_c = 3.95\ \mu$A ($Z_0 = 50\ \Omega$, $\beta_L = 1.20$, and $\omega_{LC} = 5 \times 10^{11}$ rad/s). The static flux bias is $x_e = -0.501$. (a) The conventional scheme of two-level gate operations: the microwave frequency is tuned to level separation $E_1$-$E_0$, resulting in direct transitions between the computational bases $|0\rangle$ and $|1\rangle$. (b) The same SQUID operated as a three-level $\Lambda$-SQUID qubit, where an auxiliary level, in this example the level $|4\rangle$, is used to facilitate transitions between $|0\rangle$ and $|1\rangle$.

## III. EFFECTS OF MICROWAVE PULSES

The conventional configuration of SQUID qubits utilizes the lowest level in each of the double wells (denoted as $|0\rangle$ and $|1\rangle$ in Fig. 1) as the computational basis. Unitary transformations required to accomplish one-qubit rotations, such as the Hadamard and NOT gates, are implemented by controlling the pulse area of the microwaves with frequency tuned to the level separation. The interaction between the SQUID and the microwave pulse, treated here as a linearly polarized electromagnetic field with its magnetic field component perpendicular to the plane of SQUID loop, is given by

$$V(x,t) = m\omega_{LC}^2 (x - x_e)\phi_\mu \sin\omega_\mu t + \frac{1}{2} m\omega_{LC}^2 \phi_\mu^2 \sin^2\omega_\mu t, \tag{5}$$

for $0 < t < \tau_\mu$ and zero otherwise. Here $\omega_\mu$, $\phi_\mu$, and $\tau_\mu$ are the frequency, amplitude (normalized to $\Phi_0$), and duration of the microwave pulse. The Hamiltonian of the system, $H(x,t) = H_0(x) + V(x,t)$, is now time dependent. The time evolution of the system can be obtained by numerically integrating the corresponding time-dependent Schrödinger equation (TDSE)

$$i\hbar \frac{\partial}{\partial t} \psi(x,t) = [H_0(x) + V(x,t)]\psi(x,t). \tag{6}$$

To compute the evolution of the populations on the eigenstates of the SQUID qubit, the time-dependent wave function is expanded in the eigenstates $|n\rangle$ of $H_0(x)$:

$$\psi(x,t)=\sum_{n=0}^{N} C_n(t)|n\rangle, \tag{7}$$

where $N$ is the number of eigenstates of $H_0(x)$ included in the expansion. The expansion coefficients are obtained by solving the time-dependent matrix equation

$$i\frac{\partial}{\partial\tau}C_n(\tau)=\sum_{n'=0}^{N} H^R_{nn'}(\tau)C_{n'}(\tau), \tag{8}$$

where $\tau\equiv\omega_{LC}t$ is the reduced time and the matrix elements $H^R_{nn'}$ of the reduced Hamiltonian are given by

$$H^R_{nn'}(\tau)=\frac{1}{\hbar\omega_{LC}}[E_n\delta_{nn'}+\langle n|V(x,\tau)|n'\rangle]. \tag{9}$$

Generally speaking, the expansion coefficients $C_n$ in Eq. (7) are complex and can be divided into real and imaginary parts as

$$C_n(\tau)\equiv R_n(\tau)+iS_n(\tau). \tag{10}$$

After substituting Eq. (10) into Eq. (8), we obtain a canonical equation for coefficient vectors $\mathbf{R}=\{R_n\}$ and $\mathbf{S}=\{S_n\}$, which can be expressed in matrix form as

$$\frac{d}{d\tau}\begin{pmatrix}\mathbf{R}\\ \mathbf{S}\end{pmatrix}=\begin{pmatrix}0 & \mathbf{H}\\ -\mathbf{H} & 0\end{pmatrix}\begin{pmatrix}\mathbf{R}\\ \mathbf{S}\end{pmatrix}, \tag{11}$$

where $\mathbf{H}=\{H^R_{nn'}\}$ is the reduced Hamiltonian matrix. The time evolution of the expansion coefficients can be obtained by solving the canonical equation (11) using the symplectic scheme.[25] The method is efficient and capable of providing accurate information about the dynamics of the SQUID qubit. The propagator of the second-order explicit symplectic scheme is given by

$$\mathbf{U}^k=\mathbf{R}^k+\Delta\tau\mathbf{H}^{k+1/2}\mathbf{S}^k/2,$$

$$\mathbf{S}^{k+1}=\mathbf{S}^k-\Delta\tau\mathbf{H}^{k+1/2}\mathbf{U}^k,$$

$$\mathbf{R}^{k+1}=\mathbf{U}^k+\Delta\tau\mathbf{H}^{k+1/2}\mathbf{S}^{k+1}/2, \tag{12}$$

where $\mathbf{R}^k=\mathbf{R}(\tau^k)$, $\mathbf{R}^{k+1}=\mathbf{R}(\tau^{k+1})$, $\mathbf{H}^{k+1/2}=\mathbf{H}(\tau^{k+1/2})$, and so on, and $\Delta\tau$ is the time step.

## IV. THREE-LEVEL SQUID QUBITS

Three fundamental issues of any SQUID qubit must be evaluated to asses its practical usefulness. The first is the *gate speed*. Since coupling between solid-state qubits and the environment, which results in decoherence, is inevitable, it is important to have a typical gate operation time $\tau_{\rm op}$ much smaller than the decoherence time $\tau_d$. The number of gate operations per decoherence time, $n_{\rm op}\equiv\tau_d/\tau_{\rm op}$, provides a good measure for the merit of physical qubits.[21] Considering that the decoherence time in Josephson-effect-based qubits is on the order of 1–10 $\mu$s,[17] reducing the gate time $\tau_{\rm op}$ to the order of 1 ns is essential for error-tolerant quantum computing. The second issue is the *intrinsic gate error* (IGE) rate, which measures how often the outcome of a gate operation, through pulsed microwave stimulation, produces a erroneous result. The last issue is the *leakage to noncomputational states* (LNCS)—namely, the probability of finding the qubit has leaked out of the computational bases $|0\rangle$ and $|1\rangle$ at the end of gate operations. Note that LNCS would not occur in ideal two-level qubits, but is a ubiquitous problem for qubits having more than two levels. We show that, due to the multilevel structure of the SQUID qubits, the IGE and LNCS cause significant errors even to simple one-bit SQUID quantum gate operations. Taking into account these effects results in a difficult-to-meet requirement on the speed of gate operations of the conventional two-level SQUID qubits. To circumvent the fundamental shortcomings of the 2LSQ, we propose a three-level SQUID qubit with a $\Lambda$-shaped level structure, which we call the $\Lambda$-SQUID qubit or simply $\Lambda$-Squbit. By comparing the gate operation time, IGE, and LNCS of the 2LSQ and $\Lambda$-Squbit we show that the $\Lambda$-Squbit is much faster and much less error prone than its two-level counterpart.

### A. Gate speed

For one-bit gate operations based on microwave pulse-driven Rabi oscillations, the shortest gate times are $\tau_{\rm op}=\pi/2\Omega$ and $\pi/\Omega$ for the Hadamard gate and NOT gate, respectively, where $\Omega$ is the Rabi frequency. Since the value of $\Omega$ between levels $|0\rangle$ and $|1\rangle$ is proportional to $|x_{01}|$, where $x_{01}\equiv\langle 0|x|1\rangle$ is the coupling matrix element between the two levels, it appears that one could speed up gate operations by reducing the potential barrier $\Delta U$, thus increasing $|x_{01}|$. However, this approach would not work because real SQUID's have finite damping resistance $R$ and thus finite decoherence time which decreases as the coupling matrix element increases. In fact, at low temperatures $T$, the dephasing time is proportional to $R/T$,[26,10] while the energy relaxation time from an upper level $|j\rangle$ to a lower level $|i\rangle$ is proportional to $R/|x_{ij}|^2$.[27] Hence, for a 2LSQ one has $n_{\rm op}\propto|x_{01}|^{-1}$, indicating that speeding up the gate operation through barrier reduction is actually counterproductive. It is straightforward to show that, in order to have a reasonably high value of $n_{\rm op}$, it is necessary to have at least two levels in each potential well of the SQUID.

Another option is to increase the amplitude of the microwaves because $\Omega\propto\phi_\mu$ for a weak microwave field. Here ''weak'' means roughly that $\Omega$ is much smaller than the level separation frequency $\omega_{01}$. However, this approach encounters two difficulties for the 2LSQ. First, the coupling matrix element $|x_{ij}|$ is small for levels in different wells and much larger for levels in the same well (including the delocalized levels above the barrier). Therefore, as $\phi_\mu$ is increased, the IGE and LNCS grow rapidly. In contrast, a $\Lambda$-Squbit uses the strong intrawell coupling to speed up gate operations. Figure 1(b) shows the principle of NOT operations in a $\Lambda$-Squbit. Here the logic state of the qubit is still represented by the $|0\rangle$ and $|1\rangle$ states of the SQUID. However, a rotation in the two-dimensional Hilbert space spanned by $|0\rangle$ and $|1\rangle$ is accomplished through a two-step process that involves an auxiliary state $|a\rangle$. The gate time of a $\Lambda$-Squbit, $\tau_\Lambda$, is thus the sum of

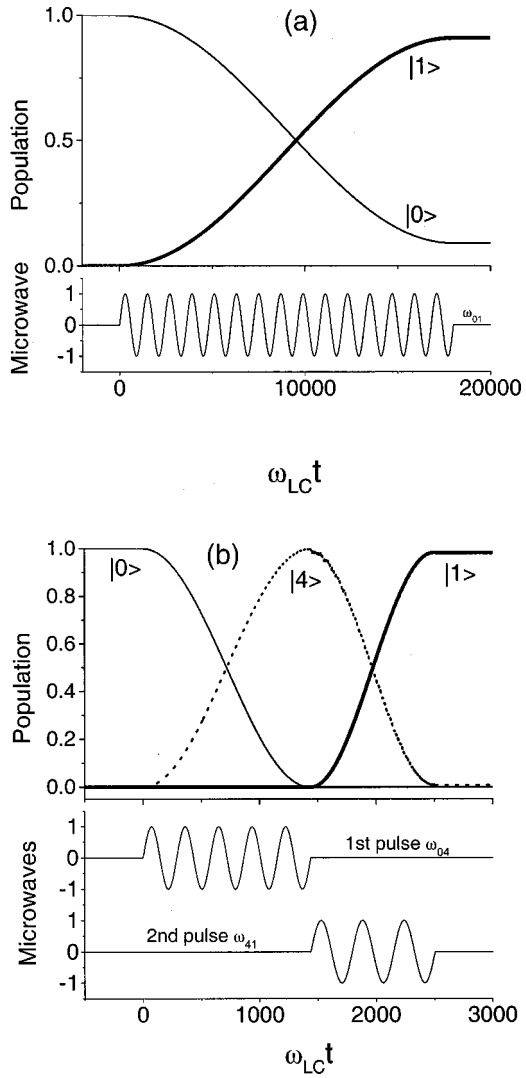


FIG. 2. Time evolution of populations on the relevant eigenstates of (a) a 2LSQ and (b) a Λ-Squbit. The SQUID parameters are the same as in Fig. 1. The time is in units of $\omega_{LC}^{-1}$. The microwave pulses are shown to illustrate the timing and pulse shape.

the times needed for transitions $|0\rangle \leftrightarrow |a\rangle$ and $|a\rangle \leftrightarrow |1\rangle$. Note that two microwave pulses of different frequencies are needed to select the desired transitions. Since NOT is one of the most common one-qubit gates and is also the foundation for realizing the two-bit CNOT, we use NOT as a benchmark for the performances of the 2LSQ and Λ-Squbit in the following discussions.

We emphasize again that the goal here is to maximize $n_{\rm op}$ and to reduce IGE and LNCS. For definitiveness, we chose $R=1\ \mathrm{M}\Omega$ in our calculations of $\tau_d$. Figure 2 shows the time evolution of the population of the relevant SQUID levels, with the same device parameters as that depicted in Fig. 1. The results are obtained by numerically solving the TDSE. In addition, $\phi_\mu = 5\times 10^{-4}$ was used for both cases. Figures 2(a) and 2(b) show the time evolution of the level population and the pulse sequence applied for the conventional 2LSQ scheme and the three-level Λ-Squbit using the level $|4\rangle$ as the auxiliary state, respectively. We emphasize that the SQUID's used for both schemes are identical. In both cases, the

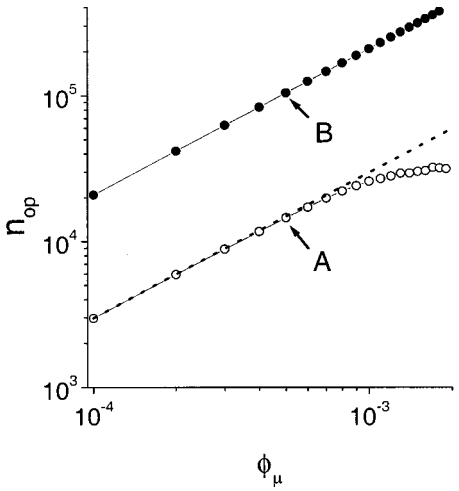


FIG. 3. Speed of NOT gates—namely, the number of operations per decoherence time $n_{\rm op}$ vs microwave intensity $\phi_\mu$ for a SQUID qubit with the same parameters as that depicted in Fig. 1. The solid circles and open circles are numerical results for the Λ-Squbit and 2LSQ, respectively. The dashed line is obtained analytically using the weak-field approximation.

SQUID is prepared in the $|0\rangle$ state at $t<0$ and a microwave pulse tuned to the relevant level separation is applied at $t=0$ as shown in the figures. The microwaves are turned off once the probability amplitude of the initial state, $C_0(t)$, reaches its first minimum. In the case of the Λ-Squbit, the process is followed by the application of a second pulse with frequency $\omega_{14}=(E_4-E_1)/\hbar$. This pulse is turned off when $C_1(t)$ reaches its first maximum. Note that the time evolution of probability amplitudes $C_{n=0,1,2,\ldots}(t)$ contains all information about the qubit, including the gate speed, IGE, and LNCS. It can be seen from the figures that the proposed Λ-Squbit is about an order of magnitude faster than its 2LSQ counterpart.

In Fig. 3 we show the calculated $n_{\rm op}$ vs $\phi_\mu$ from numerical simulations of the SQUID qubit. It is clear that for the same microwave amplitude, the gate time of the 2LSQ (open circles) is much longer than that of the Λ-Squbit (solid circles). Note that the analytical result of the weak-field approximation (dashed line) agrees well with the numerical calculations only at a very low rf field intensity. The use of different states, including the levels localized in a well and those delocalized levels above the barrier, as the auxiliary state $|a\rangle$ for the operation of a Λ-Squbit was examined. We found that the shortest gate time was achieved when the auxiliary level $|a\rangle$ is the first level above the potential barrier, in this case the level $|4\rangle$. This is expected since the gate time $\tau_\Lambda \propto |x_{0a}|^{-1}+|x_{a1}|^{-1}$ is a minimum when $|x_{0a}|=|x_{a1}|$, a condition that is most closely met by having $|4\rangle$ as the auxiliary level. Furthermore, as we will show later, significant IGE and LNCS occur at much smaller values of $\phi_\mu$ for the 2LSQ than for the Λ-Squbit. Therefore, under the constrains of the same error rate, the Λ-Squbit provides approximately an order of magnitude improvement in the speed of the NOT gate.

### B. Intrinsic gate error

Implementation of quantum algorithms requires precise gate operations. A qubit that is fast but results in significant

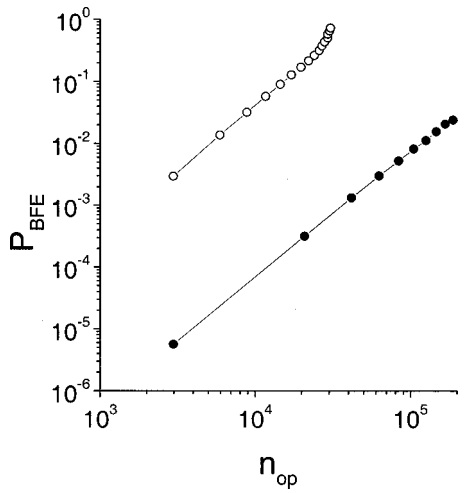


FIG. 4. Bit-flip error rate $P_{\mathrm{BFE}}$ vs gate speed $n_{\mathrm{op}}$ for the same SQUID qubit depicted in Fig. 1. The solid (open) circles are the numerical results for the Λ-Squbit (2LSQ).

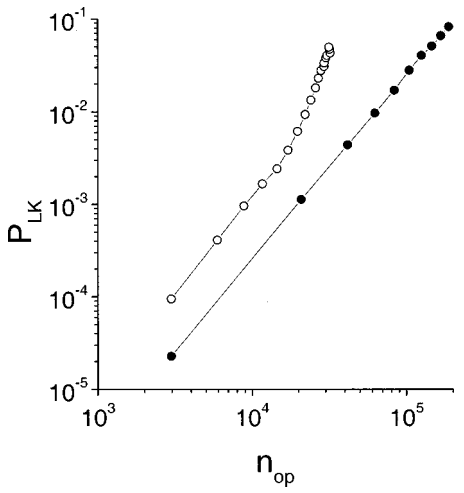


FIG. 5. Degree of leakage to noncomputational subspace $P_{LK}$ vs gate speed $n_{\mathrm{op}}$ for the same SQUID qubit depicted in Fig. 1. The solid (open) circles are the numerical results for the Λ-Squbit (2LSQ).

error, even in the ideal case of infinite decoherence time, has little value. For instance, the matrix representation of a perfect one-bit flip (NOT) operation in two-dimensional (2D) Hilbert space is one of the Pauli matrices

$$\mathrm{NOT}=\sigma_x=\begin{pmatrix}0 & 1\\ 1 & 0\end{pmatrix}. \tag{13}$$

One type of error caused by the multilevel structure of the SQUID qubit is the incomplete flip of a qubit, which results in bit-flip error (BFE) as discussed below. The corresponding matrix representation for an incomplete NOT operation on SQUID qubits can be written as

$$\mathrm{NOT}_{\mathrm{SQ}}=\frac{1}{\sqrt{1+\varepsilon^2}}\begin{pmatrix}\varepsilon & 1\\ 1 & -\varepsilon\end{pmatrix}, \tag{14}$$

where $\varepsilon \ll 1$ is assumed to be real and positive for simplicity. Although $\mathrm{NOT}_{\mathrm{SQ}}$ remains a unitary operator, it does not completely transform $|0\rangle$ to $|1\rangle$ and vice versa. For example, after the application of $\mathrm{NOT}_{\mathrm{SQ}}$ to the qubit state $|0\rangle$, the probability of finding the qubit remains in the $|0\rangle$ state is $\varepsilon^2/(1+\varepsilon^2)$. Hence it is crucial to have $\varepsilon$ as small as possible.

We investigated the bit-flip error rate $P_{\mathrm{BFE}}\equiv\varepsilon^2/(1+\varepsilon^2)$ of the conventional 2LSQ and the proposed Λ-Squbit as a function of gate speed $n_{\mathrm{op}}$ by numerically solving the TDSE as described in previous section. Figure 4 shows the value of $P_{\mathrm{BFE}}$ of the SQUID, with the same device parameters ($Z_0$, $\beta_L$, and $\omega_{LC}$) as before, operated as a 2LSQ and a Λ-Squbit with level $|4\rangle$ as the auxiliary state. Note that at the same gate speed, the bit-flip error rate $P_{\mathrm{BFE}}$ of the 2LSQ is much greater than that of its Λ-Squbit counterpart. Our results show that in the entire range of $P_{\mathrm{BFE}}$, the speed of the Λ-Squbit NOT gate is much faster than that of a 2LSQ that has an identical set of SQUID parameters as the Λ-Squbit. Because the gate error described here does not arise from decoherence due to coupling to the environment, but originates from the intrinsic energy level structure of the SQUID, we refer to it as the intrinsic gate error. Although, in principle, this type of intrinsic gate error could be eliminated by applying a sequence of carefully designed and controlled microwave pulses, the method is rather complicated.[22] The proposed Λ-Squbit utilizes only two pulses of constant intensity and thus is one of the simplest realizations of the general scheme.

### C. Leakage to noncomputational states

The last issue we want to address is the qubit state leakage—namely, a qubit started from a general state $|\psi(0)\rangle=C_0(0)|0\rangle+C_1(0)|1\rangle$ at $t=0$ with $|C_0(0)|^2+|C_1(0)|^2=1$ will "leak" to other states upon the completion of a gate operation. The amount of leakage into NCS's is characterized by the probability $P_{LK}$ of finding the qubit outside the subspace consisting of $|0\rangle$ and $|1\rangle$ at the end of a one-bit rotation (e.g., NOT). Obviously, qubits with smaller $P_{LK}$ are preferred over those having larger $P_{LK}$. We studied the leakage problem by extracting $P_{LK}$ from the time-dependent evolution of qubits after NOT operations. The result for a 2LSQ and its corresponding Λ-Squbit counterpart is presented in Fig. 5, where $P_{LK}$ is plotted as a function of gate speed (i.e., $n_{\mathrm{op}}$). Again, the Λ-Squbit has much less leakage than the conventional 2LSQ at the same gate speed. Qualitatively, the leakage is caused by coupling of the $|0\rangle$ and $|1\rangle$ to other states of the SQUID. Because the coupling strengths $|x_{02}|$ and $|x_{13}|$ are far greater than $|x_{01}|$ and the detuning is rather small for the undesired intrawell (e.g., $|0\rangle\leftrightarrow|2\rangle$) and interwell (e.g., $|1\rangle\leftrightarrow|2\rangle$ and $|2\rangle\leftrightarrow|3\rangle$) transitions, substantial population transfer to NCS's occurs at relatively low microwave intensity (hence low gate speed). As the microwave intensity is increased, cascade excitations and various multiphoton processes also become more significant, resulting in a rapid acceleration of the LNCS for the 2LSQ. In contrast, for the Λ-Squbit, the coupling strengths $|x_{04}|$ and $|x_{41}|$ are comparable to the intrawell coupling. In addition, for undesired transitions, the microwave is far off resonance (large detuning). Therefore, one expects that

LNCS presents a much smaller problem to the Λ-Squbit, which is confirmed by the result of our numerical studies presented in Fig. 5.

## V. CONCLUSION

In summary, we investigated the effects of the multilevel structure of real SQUID qubits on single-qubit gate operations. The SQUID is treated quantum mechanically, while the microwaves are treated classically. The numerical solutions of the corresponding time-dependent Schrödinger equations were obtained using a nonperturbative method. We found that due to the multilevel structure of the real SQUID's, the conventional scheme of the two-level SQUID qubit, in which the state of the qubit is assumed to be confined within the computational basis of $|0\rangle$ and $|1\rangle$, has fundamental problems such as the intrinsic gate error and leakage to the noncomputational states. Although these problems could be reduced by using very weak microwave pulses, this would significantly decrease the speed of the gates, limiting the practical usefulness of the qubits when the effect of decoherence is taken into account. Interestingly, while the SQUID's multilevel structure is largely responsible for producing IGE and LNCS in the conventional 2LSQ's, it could also be utilized to combat these problems. We showed that by adding an auxiliary level, the resulting three-level Λ-Squbit is much faster and more reliable. Therefore, the Λ-Squbit scheme significantly improves the prospects of implementing quantum computation using SQUID's.

By setting an *ad hoc* upper limit of $P_{\mathrm{BFE}}$, $P_{LK}<10^{-3}$, the shortest operation time of NOT for the Λ-Squbit is less than 3 ns compared with the 30 ns for its 2LSQ counterpart (see Figs. 4 and 5). Since the gate speed $n_{\mathrm{op}}$ of SQUID qubits is proportional to $\omega_{LC}$ for constant values of $Z_0$ and $\beta_L$, it is straightforward to increase gate speed by reducing the loop inductance and junction capacitance by the same factor and increasing the critical current to keep $\beta_L$ constant.[24] For example, SQUID's with $L=25$ pH, $C=10$ fF, and $I_c=15.8\ \mu$A will speed up the gate operation by exactly a factor of 4. SQUID's with such parameters require 0.25 $\mu$m$^2$ Nb/AlO/Nb tunnel junctions with a critical current density $J_c=6.32$ kA/cm$^2$, which are readily available with present-day Josephson tunnel junction fabrication technology.[28]

Finally, compared with the conventional 2LSQ scheme, which requires a single microwave pulse for any one-bit rotation, the proposed Λ-Squbit requires two microwave pulses of different frequencies to accomplish any one-qubit rotation. However, considering the significant improvement in the gate speed and large reduction of the intrinsic gate errors, the advantages of Λ-Squbit seem to far outweigh its drawbacks.

## ACKNOWLEDGMENTS

We thank R. Alexander for his help in preparing the manuscript. This work was supported in part by the U.S. NSF (EIA-0082499) and by AFOSR Grant No. F49620-01-1-0439 funded by the Defense University Research Initiative on Nanotechnology (DURINT) program and by ARDA. Z.Z. acknowledges partial support by the National Natural Science Foundation of China and Special Funds for Major State Basic Research Projects of China (G1999-032904).

*On leave from the Institute of Atomic and Molecular Physics, Jilin University, China.

[1] P. W. Shor, in *Proceedings of the 35th Annual Symposium on the Foundations of Computer Science*, edited by Goldwasser (IEEE Computer Society Press, Los Alamitos, CA, 1994), p. 124.

[2] D. DiVincenzo, J. Appl. Phys. **81**, 4602 (1997).

[3] S. Lloyd, Phys. Rev. Lett. **75**, 346 (1995).

[4] W. H. Zurek, Phys. Today **44**(10), 36 (1991).

[5] G. M. Palma, K. A. Suominen, and A. K. Ekert, Proc. R. Soc. London, Ser. A **452**, 567 (1996).

[6] T. P. Orlando, J. E. Mooji, Lin Tian, Caspar H. van der Wal, L. S. Levitov, Seth Lloyd, and J. J. Mazo, Phys. Rev. B **60**, 15398 (1999).

[7] F. Chiarello, Phys. Lett. A **277**, 189 (2000).

[8] A. Shnirman, G. Schön, and Z. Hermon, Phys. Rev. Lett. **79**, 2371 (1997).

[9] D. V. Averin, Solid State Commun. **105**, 659 (1998).

[10] Y. Makhlin, G. Schön, and A. Shnirman, Rev. Mod. Phys. **73**, 357 (2001).

[11] R. Rouse, S. Han, and J. E. Lukens, Phys. Rev. Lett. **75**, 1614 (1995).

[12] S. Han, R. Rouse, and J. E. Lukens, Phys. Rev. Lett. **76**, 3404 (1996).

[13] J. R. Friedman, V. Patel, W. Chen, S. K. Tolpygo, and J. E. Lukens, Nature (London) **406**, 43 (2000).

[14] C. H. van der Wal, A. C. J. ter Haar, F. K. Wilhelm, R. N. Schouten, C. J. P. M. Harmans, T. P. Orlando, Seth Lloyd, and J. E. Mooij, Science **290**, 773 (2000).

[15] D. J. Flees, S. Han, and J. E. Lukens, J. Supercond. **12**, 813 (1999).

[16] Y. Nakamura, Y. A. Pashkin, and J. S. Tsai, Nature (London) **398**, 786 (1999).

[17] S. Han, Y. Yu, X. Chu, S.-I. Chu, and Z. Wang, Science **293**, 1457 (2001).

[18] J. I. Cirac and P. Zoller, Phys. Rev. Lett. **74**, 4091 (1995).

[19] J. A. Jones, M. Mosca, and R. H. Hansen, Nature (London) **393**, 344 (1998).

[20] T. Pellizzari, S. A. Gardiner, J. I. Cirac, and P. Zoller, Phys. Rev. Lett. **75**, 3788 (1995).

[21] M. A. Nielsen and I. L. Chuang, *Quantum Computation and Quantum Information*, 1st ed. (Cambridge University Press, Cambridge, UK, 2000), Chap. 7.

[22] L. Tian and S. Lloyd, Phys. Rev. A **62**, 050301(R) (2000).

[23] V. V. Danilov, K. Likharev, and A. B. Zorin, IEEE Trans. Magn. **19**, 572 (1983).

[24] Y. Yu, S. Han, X. Chu, S.-I. Chu, and Z. Wang, Science **296**, 889 (2002).

[25] Z. Zhou, P. Ding, and S. Pan, J. Korean Phys. Soc. **32**, 417 (1998).

[26] A. J. Leggett, S. Chakravarty, A. T. Dorsey, M. P. A. Fisher, A. Garg, and W. Zwerger, Rev. Mod. Phys. **59**, 1 (1987).

[27] A. I. Larkin and Y. N. Ovchinnikov, Sov. Phys. JETP **64**, 185 (1986).

[28] Z. Bao, M. Bhushan, S. Han, and J. Lukens, IEEE Trans. Appl. Supercond. **5**, 2731 (1995).